# Localization of electrons in ionic liquids: Nuclear magnetic resonance in Cs-CsI and CsI-I solutions

William W. Warren, Jr., S. Sotier,* and G. F. Brennert
*AT&T Bell Laboratories, Murray Hill, New Jersey 07974*
(Received 14 December 1983)

We describe a $^{133}Cs$ and $^{127}I$ nuclear-magnetic-resonance investigation of liquid solutions in the system Cs-CsI-I. Measurements of the resonance shifts and nuclear relaxation rates were carried out as functions of composition and, to a limited extent, of temperature. Excess electrons introduced by dilute amounts of Cs in CsI were found to be localized on the time scale of the underlying liquid structure. The spatial distribution of these states is represented well by *F*-center analogs. Excess I in CsI produces paramagnetic centers which are analogs of $V_K$ centers, i.e., $I_2^-$ molecular ions. Addition of higher concentrations of Cs to CsI rapidly increases the electronic mobility and the system passes through a continuous metal-nonmetal transition in the range 5—20 at. % excess Cs. On the metallic side of the transition, electronic transport is initially of strong-scattering diffusive character which gives way to nearly-free-electron conditions when the Cs content exceeds about 60 at. %. High concentrations of I in CsI lead to increased concentrations of localized paramagnetic species.

## I. INTRODUCTION

Interest in the metal-nonmetal transition has motivated experimental study of a number of systems in which the conduction-electron density can be varied over a wide range. Some familiar examples include highly doped semiconductors, liquid-metal—ammonia and related solutions, expanded liquid metals, and co-deposited metal-nonmetal amorphous films.[1] Liquid solutions of alkali metals and their molten halides have the interesting property that the ratio of electrons to metal ions rather than the "donor" concentration varies with composition. Thus, as is also true of highly compensated semiconductors, intraionic electron-electron—interaction effects are not expected to be important in the range of low electron density. For some systems and temperature ranges, the electron/ion ratio may be varied over the full range from 1 to 0, giving a continuous transition from the nearly-free-electron liquid alkali metal to the highly-charge-ordered ionic liquid. In other cases, liquid-liquid phase separation intervenes.[2] Charge transfer from the metal to the halogen is a dominant characteristic of alkali halides and, consequently, the alkali-metal—alkali-halide solutions are prototypes of a more general class which includes the so-called "ionic alloys" or "charge-transfer insulators." These systems, exemplified by cesium-gold alloys,[3,4] form ionic compounds at a particular stoichiometry such as $Cs_{0.5}Au_{0.5}$.

The phase diagrams and electrical properties of alkali-metal—alkali-halide solutions were extensively studied in a series of pioneering investigations by Bredig and co-workers. This work and subsequent investigations have been summarized in several reviews.[2,5,6] A central problem raised by the early studies concerns the nature of the electronic states for low concentrations of metal in the molten halide. Here, a low density of conduction electrons experiences a strong, unscreened ionic potential having a high degree of short-range compositional order. Considerable controversy has developed over the existence and properties of localized electronic states in this range.[7] The opposite limit, the impurity state of the highly electronegative halogen in an alkali metal, was studied in detail by Flynn and co-workers.[8—10] They found that the conduction-electron system is strongly perturbed by the negative ion and the resultant screening leads to greatly enhanced impurity diamagnetism.

Among the alkali-metal—alkali-halide solutions, the cesium—cesium-halide solutions have the special property that no liquid-liquid phase separation occurs and the solutions are homogeneous throughout the liquid range.[2] The continuous metal-nonmetal transition may therefore be studied without the experimental complications introduced by high critical points for phase separation. A number of physical properties have been measured for the cesium—cesium-halide solutions, including electrical conductivity [Cs-CsCl (Ref. 11) and Cs-CsI (Ref. 12)], magnetic susceptibility [Cs-CsCl and Cs-CsI (Refs. 11 and 13)], optical-absorption spectra at low metal concentrations [Cs-CsCl (Refs. 14—16) and Cs-CsI (Ref. 16)], optical reflectivity [Cs-CsCl (Ref. 17)], and heats of mixing [Cs-CsF, Cs-CsCl, and CsCsI (Refs. 18 and 19)]. Such studies have yielded a great deal of useful information about these solutions, but have not revealed the microscopic structure and dynamic properties of the electronic states.

The alkali iodides also form homogeneous liquid solutions with elemental iodine[20] and thus exhibit continuous transitions from the ionic molten salt to the molecular insulator $I_2$. In analogy to the dilute solutions of metal in the molten halide, dilute solutions of iodine present the possibility of localized electronic states associated with the excess iodine. At higher concentrations of iodine, the presence of polyiodide anionic species has been proposed.[20] There are few previous studies of the physical properties of the alkali-halide—iodine solutions over wide concentration ranges. However, the magnetic susceptibili-

 

ty of CsI-I has been measured recently over the full range of concentrations and electron-spin-resonance (ESR) and optical-absorption spectra were obtained for dilute I in molten CsI.[21]

This paper describes a nuclear-magnetic-resonance (NMR) investigation of Cs-CsI-I liquid solutions from 60 at. % excess Cs in CsI to 50 at. % excess I. The principal focus of the work is the use of the nuclear hyperfine interaction to probe the microscopic structure and dynamics of electron states associated with excess metal and excess iodine in CsI. We have measured the $^{133}$Cs and, where possible, the $^{127}$I nuclear-spin-relaxation rates and resonance shifts. The composition and temperature ranges investigated are indicated in the Cs-I phase diagram reproduced in Fig. 1. Preliminary, partial reports of this work have been published previously.[22–25]

Specifically, the investigation addressed the following questions which we consider central to the understanding of these solutions. First, what is the state of the excess electrons associated with low concentrations of Cs in CsI? Do these electrons form a low-density metal or do they localize? If the latter is the case, what are the structural and dynamic properties of these states? Second, and complementary to the first, what can be said about the state of I dissolved in liquid Cs? Third, we consider how electrons are transported at low concentrations of Cs in CsI and study the changes in transport on passing through the metal-nonmetal transition. What can be inferred about the liquid structure in the transition range? Finally, in the CsI-I range, what kinds of associated species occur in these nonmetallic solutions. What are the magnetic properties of states associated with excess I in CsI?

The organization of this paper is as follows. Section II contains a condensed summary of the NMR theory used to relate our experimental results to the questions raised in the preceding paragraph. In Sec. III we describe our experimental techniques, and in Sec. IV we present the experimental results. Analysis and interpretive discussion of the experiments may be found in Sec. V. Finally, in Sec. VI we present a summary of the main conclusions of the work.

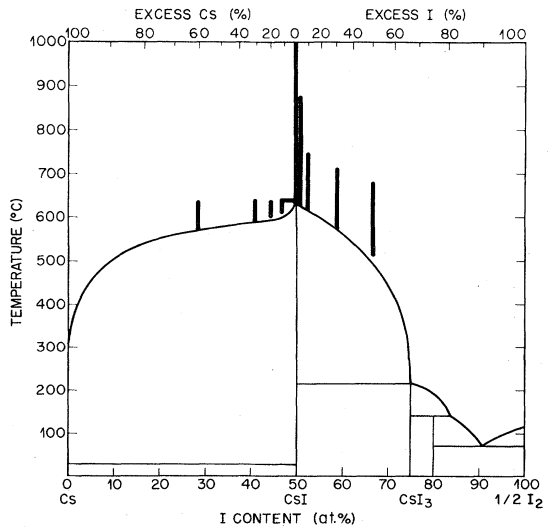


FIG. 1. Temperature-composition phase diagram for the Cs-I system. Thick solid lines indicate temperature and composition ranges covered in this investigation. Upper scale shows excess-Cs—excess-I designation adopted in this paper.

## II. THEORY

The quantities measured in these experiments are the resonance shift $\Delta H$, the nuclear-spin-lattice relaxation time $T_1$, and the free-induction decay lifetime $T_2^*$. These quantities reflect the local environment of the resonant nuclei through the influence of two dominant interactions, the scalar magnetic hyperfine interaction with spins of unpaired electrons and the nuclear electric quadrupole interaction related to neighboring ionic and electronic charges. We shall show later that the effects of coupling to orbital diamagnetism and the nuclear dipole-dipole coupling are small or completely negligible compared with those due to the hyperfine and quadrupole interactions.

### A. Magnetic hyperfine interaction

The basic Hamiltonian for a set of nuclear spins $\vec{I}^{\,i}$ in an applied field $H_0$ and coupled to electrons $\vec{S}^{\,j}$ is written as

$$\mathcal{H}=\gamma_n\hbar\sum_i I_z^i H_0+\sum_{i,j}A_{ij}(t)\vec{I}^{\,i}\cdot\vec{S}^{\,j}\,, \tag{1}$$

where $\gamma_n$ is the nuclear gyromagnetic ratio and $A_{ij}(t)$ is the (time-dependent) scalar hyperfine coupling. The first term in Eq. (1) is, of course, the nuclear Zeeman interaction responsible for the NMR effect itself, and the second term is the magnetic hyperfine perturbation responsible for shifts and relaxation phenomena.

The shift, measured relative to the resonance position of a specified diamagnetic reference material, is given by

$$\frac{\Delta H}{H_0}=\frac{H_{\rm ref}-H_0}{H_0}=(N_0\gamma_e\gamma_n\hbar^2)^{-1}\langle A\rangle\chi_m^{e,p}\,, \tag{2}$$

where $\gamma_e$ is the electronic gyromagnetic ratio, $\chi_m^{e,p}$ is the contribution to the molar susceptibility from electronic paramagnetism, and the average hyperfine coupling $\langle A\rangle$ is related to the electron probability amplitude at the resonant nuclear site $\vec{R}_i$,

$$\langle A\rangle=\frac{8\pi}{3}\gamma_e\gamma_n\hbar^2\langle\,|\Psi(\vec{R}_i)|^2\rangle\,. \tag{3}$$

In a metal, $\chi_m^{e,p}$ is the Pauli susceptibility enhanced by electron-electron interactions and density-of-states effects. Equation (2) then describes the Knight shift,[26]

$$K=\frac{\Delta H}{H_0}=\frac{8\pi}{3}\langle\,|\Psi(R_i)|^2\rangle_F\chi_a^P\,, \tag{4}$$

where the average $\langle\ \rangle_F$ now includes an average over all electron states at the Fermi energy and $\chi_a^P$ is the enhanced Pauli susceptibility per atom. In the localized limit, a mole fraction $c_s$ of spins $S=\frac{1}{2}$ yields a Curie susceptibility

$$\chi_m^C=\frac{c_s N_0\gamma_e^2\hbar^2}{4kT}\,, \tag{5}$$

and a shift

$$\frac{\Delta H}{H}=\frac{c_s}{4kT}\left[\frac{\gamma_e}{\gamma_n}\right]\langle A\rangle\ . \tag{6}$$

The relaxation effects are governed by an autocorrelation function for transverse components of the hyperfine field,[27]

$$G_{\pm}(t)=\tfrac{1}{4}\left\langle \sum_{i,j} A_{ij}(t)S^j_{+}(t)A_{ij}(0)S^j_{-}(0)\right\rangle\ , \tag{7}$$

where, as usual, $S_{\pm}=S_x\pm iS_y$. The spin-lattice or longitudinal relaxation rate is then

$$\frac{1}{T_1}=\frac{2}{\hbar^2}\int_{-\infty}^{\infty} dt\, e^{-i\omega_0 t}G_{\pm}(t)\ , \tag{8}$$

in which $\omega_0$ is the nuclear Larmor frequency $\gamma_n H_0$. The time dependence of the local-field fluctuations can be characterized by a correlation time $\tau$ defined by assuming an exponential decay for $G_{\pm}(t)$,

$$G_{\pm}(t)=G_{\pm}(0)e^{-t/\tau}\ . \tag{9}$$

In a liquid the ionic and electronic fluctuations are often rapid compared with the electron Larmor frequency $\omega_e=\gamma_e H_0$. In this case, i.e., when $\omega_e\tau\ll 1$, the transverse relaxation time $T_2$ equals $T_1$. If, in addition, static inhomogeneities are negligible, then $T_1=T_2=T_2^*$. This is an important experimental consideration since for very short relaxation times, it is often substantially easier to measure $T_2^*$ than $T_1$.

For a metal described by the nearly-free-electron model in the absence of electron-electron interactions, evaluation of Eqs. (4), (7), and (8) leads to the Korringa relaxation rate[28]

$$\left[\frac{1}{T_1}\right]_{\text{Korringa}}=\frac{4\pi kT}{\hbar}\left[\frac{\gamma_n}{\gamma_e}\right]^2 K^2\ . \tag{10}$$

The Korringa rate is a good rough approximation to the relaxation rate for simple metals, but there are important corrections. Electron-electron interactions typically reduce the actual rate relative to $(1/T_1)_{\text{Korringa}}$. For example, in liquid Cs below about 800 °C, $\eta\equiv(1/T_1)/(1/T_1)_{\text{Korringa}}\simeq 0.6$.[29] Another important effect results from the strong electron-ion interactions encountered upon approaching the metal-nonmetal transition in a disordered system. The rate becomes enhanced as electrons begin to spend more time near individual nuclei. The enhancement is given by the approximate relation[30]

$$\eta\simeq\tau/\hbar N_e(E_F)\ , \tag{11}$$

where $N_e(E_F)$ is the density of states per electron at the Fermi energy. The right-hand side of Eq. (11) is of order 1 under nearly-free-electron conditions so that the Korringa relation is recovered. The observation that $\eta\gg 1$, on the other hand, gives a direct experimental indication of the breakdown of nearly-free-electron conditions and the tendency toward localization.

In the highly localized limit the relaxation rate is given by[27]

$$\frac{1}{T_1}=\frac{c_s}{2\hbar^2}\langle A^2\rangle\tau\ . \tag{12}$$

Whereas the correlation time in the metallic limit is related to the translational motion of the conduction electrons past a nucleus, i.e., fluctuations of $A_{ij}(t)$ in Eq. (7), $\tau$ in the localized limit may be characteristic either of fluctuations of the coupling $A_{ij}(t)$ or spin fluctuations $\vec{S}^j(t)$, whichever are faster. Later we shall argue, in fact, that coupling fluctuations dominate at all concentrations in Cs-CsI solutions.

### B. Electric quadrupolar interactions

For nuclei with $I>\frac{1}{2}$, the nuclear electric quadrupolar interaction must be considered. The additional term in the Hamiltonian of Eq. (1) is

$$\mathcal{H}_Q(t)=\sum_{m=-2}^{2} Q^m V^{-m}(t)\ , \tag{13}$$

where $Q^m$ and $V^{-m}$ are symmetrized combinations of spin operators and electric-field-gradient components, respectively.[31] The time dependence comes from relative motions of the resonant nuclei and neighboring charges. Because the quadrupole interaction vanishes in first order for a spherically symmetric charge distribution, the rapid motions characteristic of most liquids lead to vanishing quadrupolar splittings. However, the mean-square fluctuation gives rise to a relaxation process which can dominate the nuclear relaxation in some cases. In analogy to the magnetic hyperfine relaxation process, the rate is governed by Fourier transforms of correlation functions for the fluctuating electric field gradient,

$$J_m^Q(m\omega_0)=\int_{-\infty}^{\infty} dt\, e^{-im\omega_0 t}\langle V^m(t)V^{-m}(0)\rangle\ . \tag{14}$$

In all but the most viscous liquids, the fluctuations are rapid compared with the nuclear frequency $\omega_0$ and the rate is given by[32]

$$\left[\frac{1}{T_1}\right]_Q=\left[\frac{1}{T_2}\right]_Q=(\tfrac{3}{4})f(I)\left[\frac{eQ}{\hbar}\right]^2 J^Q(0)\ , \tag{15}$$

where

$$f(I)=(2I+3)/I^2(2I-1)$$

and $Q$ is the nuclear quadrupole moment. For $^{127}$I, $Q=-0.79\times10^{-24}$ cm$^2$ compared with $-0.003\times10^{-24}$ cm$^2$ for $^{133}$Cs.[33] Thus even without taking into account the spin factor $f(I)$ we can see that quadrupolar relaxation is much more important for $^{127}$I than $^{133}$Cs.

In the general case of a dissociated liquid such as a molten alkali halide, the fluctuating field gradients are determined by the complex vibrational and translational motions of individual ions. No rigorous theory for $J^Q(0)$ exists for a dissociated liquid. A simpler special case applies for stable molecular or polyatomic ions (e.g., $NO_3^-$) where the rotational motion can be described by a diffusion equation. In this case a rotational correlation time $\tau_r$ can be defined and the relaxation rates become[32]

$$\left[\frac{1}{T_1}\right]_Q = \left[\frac{1}{T_2}\right]_Q = \left(\tfrac{3}{40}\right) f(I) \left[1+\frac{\sigma^2}{3}\right] \left[\frac{e^2qQ}{\hbar}\right]^2 \tau_r \ , \tag{16}$$

where $q$ and $\sigma$ are the principal component and asymmetry parameter, respectively, for the electric-field-gradient tensor defined in the molecular coordinate system.

The dependence of the rates on the factor $f(I)Q^2$ provides a means of establishing whether quadrupolar relaxation is responsible for an observed process in the special case where measurements can be made for two isotopes of the same element. Thus the ratio of the quadrupolar rates for isotopes $A$ and $B$ will be

$$(1/T_1)_A/(1/T_1)_B = f(I_A)Q_A^2/f(I_B)Q_B^2 \ . \tag{17}$$

In contrast, if a magnetic process such as that of Eqs. (7) and (8) dominates, the ratio is

$$(1/T_1)_A/(1/T_1)_B = (\gamma_A/\gamma_B)^2 \ . \tag{18}$$

While this method cannot be employed for Cs and I since only a single isotope is stable for each element, we will describe a supplemental experiment involving the use of $^{85}$Rb and $^{87}$Rb to identify the relaxation mechanism in an analogous solution containing RbI.

### C. Orbital diamagnetism—chemical shifts

Diamagnetism of the total electron charge distribution produces small differences in the resonant field in different chemical compounds even in the absence of unpaired electrons.[34] Compared with the paramagnetic shifts of Eq. (2), chemical shifts are negligible except for very low spin concentrations. In this case we must take into account the chemical shift relative to our reference material for an accurate evaluation of the paramagnetic shift.

### D. Dipole-dipole interactions

Nuclear dipole-dipole couplings lead to a relaxation process which might, in principle, compete with the magnetic hyperfine and electric quadrupole processes discussed above. However, estimates of the rates for $^{133}$Cs and $^{127}$I yield values $(1/T_1)_{DD} \sim 10^{-4}$ s$^{-1}$. This is 3 orders of magnitude lower than the smallest rates measured in this study ($1/T_1 \sim 10^{-1}$ s$^{-1}$ for $^{133}$Cs in molten CsI). Thus we will neglect dipolar interactions in interpreting our experimental results.

## III. EXPERIMENTAL METHODS

The samples used in these experiments were prepared from CsI (purity $>99.99\%$) which we dried by pumping on the powdered material at 500 °C. The dried CsI and appropriate amounts of Cs metal or $I_2$ were loaded and sealed in the experimental cells without subsequent exposure to the atmosphere.

We used two different cell types depending on the composition range of the sample. For pure CsI and solutions in the excess I range (CsI-I) we used fused-silica ampoules in which the samples were sealed under vacuum. These cells were unsuitable for solutions containing excess Cs because of the strong chemical reaction between Cs and silica at the experimental temperatures. For such samples we employed $Al_2O_3$ (alumina ceramic or sapphire) cells[35] which were closed with a Nb-Nb cone seal. The achievement of a vacuum-tight Nb—$Al_2O_3$ bond sealing the closure assembly to the cell was the most difficult aspect of these experiments. The most successful bonds were obtained with Ni-Ti brazing alloys. After sealing the closure assembly to the cell and testing for the absence of leaks, we loaded the cells and closed the cone seal in the helium atmosphere of a dry box. We made no attempt to subdivide the material into small droplets and the NMR signal was therefore obtained only from nuclei within the radio-frequency skin depth.

The $Al_2O_3$—Nb bonds eventually began to leak after exposure to Cs vapor for a few hours at temperatures above 600 °C. In some cases the loss of Cs was sufficiently slow that we could continue to take data for several days. Using the shift as an indicator of the drifting composition we interpolated between measurements of stable compositions in tight cells to assign compositions to relaxation-rate data.

The required high-temperature sample environments were obtained in furnaces heated by noninductively wound resistive elements carrying regulated dc currents. A single coil for NMR was located inside the heater element and fit snugly around the sample cell. Depending on the cell type required, we used one of two different furnaces. For samples in fused silica, the furnace was based on a Pt heating element and NMR coil and operated in an air atmosphere. This hot-air environment is unsuitable for the Nb—$Al_2O_3$ cells, however, because of rapid oxidation of Nb at high temperatures. For these cells we used a furnace which can be closed against the atmosphere and which, for these experiments, contained 1—2 atm of argon gas. The element and NMR coil in this furnace are made of Mo which is resistant to attack by leaking Cs vapor. In the air-atmosphere furnace, sample temperatures could be measured with an accuracy of 5 °C using Pt—Pt-10 at. % Rh thermocouples, while in the controlled-atmosphere furnace-temperature errors could be as large as 10 °C.

The NMR measurements were carried out with a coherent transient NMR spectrometer operating at 9.7 MHz. By sweeping the magnetic field while integrating most of the free-induction decay with a boxcar integrator we obtained a resonance profile suitable for shift measurements.[36] The reference samples for shift determinations were aqueous solutions of CsCl and KI, corrected to infinite dilution, for $^{133}$Cs and $^{127}$I, respectively.

Spin-lattice relaxation times ($T_1$) were normally measured with a standard $\pi - \pi/2$ pulse sequence. The exception to this was the case of pure CsI, for which the relaxation times are so long ($\sim 10$ s) that a saturating-train $-\pi/2$ sequence was more efficient. For the shortest relaxation times encountered, those in the range 27—60 $\mu$s, it was more convenient and accurate to measure the free-induction decay lifetime $T_2^*$. We verified directly that $T_2^* = T_1$ at a single composition of Cs-CsI.

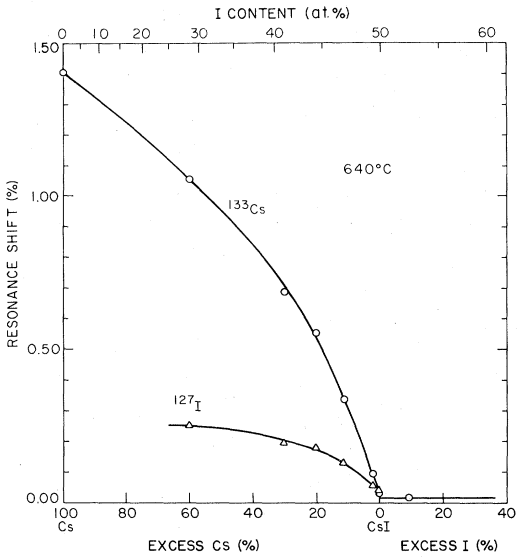


FIG. 2. Resonance shifts vs composition for $^{133}$Cs (circles) and $^{127}$I (triangles) in liquid Cs-CsI-I solutions at 640 °C.

## IV. EXPERIMENTAL RESULTS

### A. Resonance shifts

The composition dependences of the resonance shifts at 640 °C for $^{133}$Cs and $^{127}$I are presented in Fig. 2. The $^{133}$Cs shift decreases monotonically but nonlinearly from the large Knight shift[29] of pure liquid Cs [(1.398±0.003)%] to the small chemical shift of molten CsI [(0.034±0.002)%]. There is little further change of shift for excess I in CsI.

The $^{127}$I shift follows a similar composition dependence but it is substantially smaller in magnitude than the $^{133}$Cs shift. A rough extrapolation suggests that the $^{127}$I shift should be about 20% of the $^{133}$Cs Knight shift for dilute I in liquid Cs. These observations show that while the excess electrons couple much more strongly to the Cs nuclei than to I, a substantial spin density remains at the I nuclei even in very metallic solutions. Except for our most dilute sample of excess I in CsI ($<1$ at. %), we were unable to observe the $^{127}$I NMR in the excess-I range. Even in the dilute case, the resonance line was so broad that a shift measurement was impractical.

The temperature range of our measurements on samples containing excess Cs was severely limited by increasing difficulties with leaking cell seals above about 650 °C. However, data taken between the liquidus and 650 °C established that the $^{133}$Cs shift tends to increase with increasing temperature in all the solutions. Representative values of the coefficient $\partial \ln(\Delta H)/\partial T$ are given in Table I. There is a substantial increase in $\partial \ln(\Delta H)/\partial T$ as the excess Cs content is reduced to 30 at. % or less.

TABLE I. Temperature dependence of the $^{133}$Cs resonance shift in $Cs_x(CsI)_{1-x}$ solutions.

| $x$ | $K$(640 °C) (%) | $\partial \ln(\Delta H)/\partial T$ ($10^{-4}$ K$^{-1}$) |
|---|---|---|
| 1.00 | 1.398±0.003 | 0.0±0.4 |
| 0.60 | 1.055±0.005 | 1.9±1.0 |
| 0.30 | 0.688±0.010 | 16±3 |
| 0.20 | 0.555±0.010 | 16±2 |
| 0.11 | 0.337±0.010 | 13±3 |

### B. Nuclear relaxation rates

Nuclear relaxation rates $1/T_1$ and $1/T_2$ for $^{133}$Cs and $^{127}$I are shown in Fig. 3 plotted against composition at 640 °C. Although the $^{133}$Cs rate initially decreases on adding CsI to Cs, the rate rises rapidly at lower concentrations and exhibits a sharp peak around 5 at. % excess Cs. On the linear scale of Fig. 3, the rates for pure-CsI and excess-I solutions are vanishingly small.

The $^{127}$I rates exhibit a similar, although smaller, peak in the Cs-CsI solutions. The $^{127}$I relaxation rate in pure CsI is substantially higher than the $^{133}$Cs rate and addition of less than 1 at. % excess I produces a rapid increase in $1/T_2^*$ (not shown in Fig. 3). This line-broadening effect is so strong that we were unable to observe the $^{127}$I NMR except in our most dilute excess-I sample where the rate is $1/T_2^* = (6.7\pm0.9)\times10^4$ s$^{-1}$ at 640 °C.

The full range of relaxation rates for $^{133}$Cs is displayed in Fig. 4 which shows $1/T_1$ and $1/T_2^*$ plotted semilogarithmically against composition. The extreme sensitivity of the $^{133}$Cs rate to small additions of Cs or I to CsI is clearly evident in this plot. For example, addition of only 0.5 at. % excess Cs produces an enhancement of the relaxation rate of more than 5 orders of magnitude. The corresponding effect is smaller for excess I but an increase of more than 2 orders of magnitude is observed for a 2-at. % addition. The sharp relaxation-rate peak characteristic of

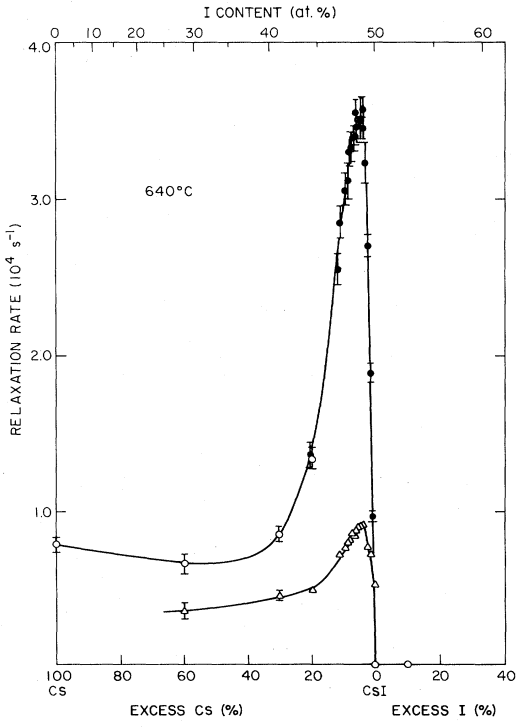


FIG. 3. Nuclear relaxation rates vs composition for $^{133}$Cs (circles) and $^{127}$I (triangles) in liquid Cs-CsI-I solutions at 640 °C. Open points denote $1/T_1$ values; solid points denote $1/T_2^*$.

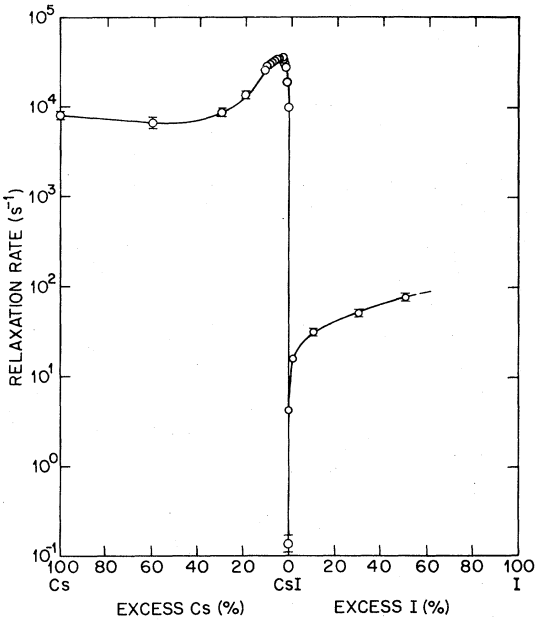


FIG. 4. Semilogarithmic plot of $^{133}$Cs nuclear relaxation rates ($1/T_1$ and $1/T_2^*$) vs composition in liquid Cs-CsI-I solutions at 640°C.

excess-Cs solutions is absent in the excess-I range.

Stability of the samples in fused-silica ampoules permitted us to measure the temperature dependence of $1/T_1$ for $^{133}$Cs in CsI and in the excess-I range CsI-I. These results are presented in a semilogarithmic plot of $1/T_1$ against $1/T$ in Fig. 5. The very low relaxation rate in pure liquid CsI at the melting point tends initially to decrease further upon heating, but above about 850°C it rises rapidly. This effect may indicate decomposition, producing very small amounts of excess Cs, i.e., $2CsI \rightarrow 2Cs + I_2$, or, alternatively, a weak reaction may develop between the CsI and the silica container. The initial negative temperature dependence just above the melting point is similar to the quadrupolar relaxation typically observed for other molten alkali halides.[37]

For excess I solutions CsI-I, $1/T_1$ increases rapidly with increasing temperature. The temperature dependence, expressed as an activation energy $\Delta E$, tends to increase with increasing I content (inset of Fig. 5).

Because only one isotope is available each for Cs and I, we cannot employ Eqs. (17) and (18) to identify the relaxation mechanism in Cs-CsI-I solutions. However, the small value of $Q$ for $^{133}$Cs excludes quadrupolar relaxation as the strong process responsible for the relaxation peak in Cs-CsI. To see this it is sufficient to compare the greater strength of the observed $^{133}$Cs rates in this range with those of $^{127}$I. If the $^{133}$Cs relaxation were quadrupolar, the $^{127}$I rates should exceed the $^{133}$Cs rates by a large factor. Moreover, comparison of the data for pure CsI with those for other molten alkali halides[37] strongly suggests that both species are relaxed by the quadrupolar process in the pure salt. This rate should not change dramatically with small additions of excess metal.

As an aid to identification of the relaxation mechanism in excess-I solutions, we measured $1/T_1$ for $^{85}$Rb and $^{87}$Rb in $(RbI)_{0.33}I_{0.67}$ ("$RbI_3$"). (The phase diagrams of RbI-I and CsI-I are very similar.[20]) The results are shown plotted against temperature in Fig. 6. Note that for a quadrupolar process for these isotopes, Eq. (17) predicts $(1/T_1)_{85}/(1/T_1)_{87} = 1.025$, while for a magnetic process the ratio is 0.0871. It is immediately evident from Fig. 6 that the rates are comparable for the two isotopes, thus establishing that quadrupolar relaxation is dominant and decreases slowly with temperature. At the highest temperatures, however, a relative increase in the rate for $^{87}$Rb signals the appearance of a weaker magnetic process which increases with temperature. Upon decomposition of the rates to separate the two contributions using Eqs.

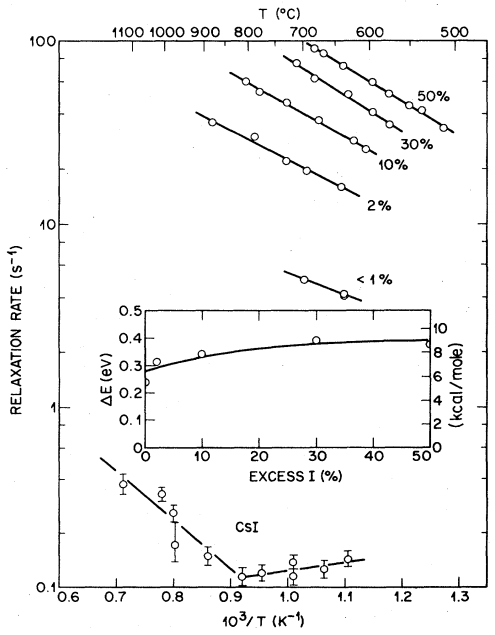


FIG. 5. Semilogarithmic plot of $^{133}$Cs nuclear-spin-lattice relaxation rates vs inverse temperature for CsI and CsI-I solutions. Excess iodine concentrations are indicated. Inset: activation energy of relaxation rate ($\Delta E$) vs excess iodine concentration.

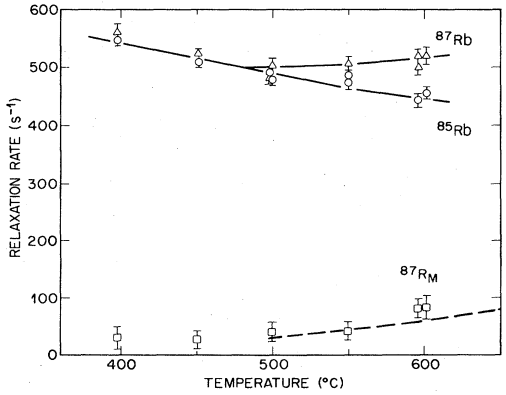


FIG. 6. Upper: Nuclear-spin-lattice relaxation rates vs temperature for $^{85}$Rb (circles) and $^{87}$Rb (triangles) in $(RbI)_{0.33}I_{0.67}$. Lower: $^{87}$Rb magnetic relaxation rate (squares) compared with $^{133}$Cs rate in $(CsI)_{0.5}I_{0.5}$ indicated by dashed line.

(17) and (18), we find that the magnetic process for $^{87}Rb$ has roughly the same magnitude and temperature dependence as the total relaxation observed for $^{133}Cs$ in $(CsI)_{0.50}I_{0.50}$. This is strong evidence that the dominant process in CsI-I solutions is of magnetic origin.

## V. ANALYSIS AND INTERPRETATION

### A. Cs-CsI solutions

#### *1. Description of liquid structure*

To provide a basis for discussion of the electronic properties of Cs-CsI solutions we briefly summarize what is known of the liquid structure from scattering experiments and computer simulations.

Pure molten alkali halides are characterized by a high degree of local compositional order extending over several neighbor shells.[38] The local configuration strongly resembles that of the crystal in the sense that an anion has a high probability of being surrounded mainly by cations and vice versa. First-neighbor coordination numbers in the range 4 to 6 are generally observed. The exact value depends on the method used to integrate the first peak in the partial pair distribution function.[39] A careful study of NaCl by Edwards *et al.*,[40] recently reevaluated by Biggin and Enderby,[39] yields a value of 4.5 for the average number of cations around an anion. Derrien and Dupuy found a first-neighbor coordination number of 6.0 for CsCl.[41] The partial pair distribution functions also reveal the imperfection of the compositional order expressed as small but measurable "penetration" of like species into the first-neighbor sphere of predominantly unlike species.[38]

Pure liquid cesium also has a relatively low first-neighbor coordination number compared with typical close-packed liquids. Near the melting point a value $n_1 \simeq 9$ for cesium has been reported.[42] Although the coordination number has not been determined over a wide range of temperature, we can estimate a value from neutron-diffraction results reported for liquid rubidium.[43] It was found that the value of $n_1$ for liquid rubidium decreases roughly in proportion to the density as the temperature is raised. Assuming the same dependence for liquid cesium, we estimate $n_1 \sim 7$ at 640 °C, the temperature of our studies of Cs-CsI solutions.

Neutron measurements of the partial pair distribution functions in K-KCl indicate a saltlike arrangement around the anion, even for a highly metal-rich solution, $K_{0.80}(KCl)_{0.20}$.[44] The number of first-neighbor $K^+$ ions around a $Cl^-$ ion was found to be about 4 and a $(K_5Cl)^{4+}$ complex was suggested. Thermodynamic studies[18,19] of cesium-cesium halides provide additional but indirect evidence for a complex associated with the anion in metal-rich solutions. We can assume with some confidence, therefore, that I is ionized and coordinated with an average of four to six $Cs^+$ ions in the Cs-CsI solutions we have investigated.

The foregoing information leads us to a picture of the Cs-CsI solutions as assemblies of $Cs^+$ and $I^-$ ions lacking long-range order but maintaining nearly the maximum short-range compositional order compatible with the Cs concentration. Within this structure the conduction or excess electrons have an average density proportional to the atomic fraction of excess metal $x$, i.e., $n_e = xN_0/\Omega_m$ where $\Omega_m$ is the molar volume of a solution $Cs_x(CsI)_{1-x}$. For $x = 1$, the electrons form the nearly-free-electron (NFE) gas typical of pure alkali metals. We must now consider the states of these electrons as $x$ decreases toward zero.

#### *2. Destruction of the NFE metal: Korringa relation*

Approximate validity of the Korringa relation, Eq. (10), modified by electron-electron effects, is a good test for a NFE metal. The relaxation rates in elemental liquid metals generally fall within a factor of 2 of the Korringa value determined from their Knight shifts.[45] For liquid Cs in the low-temperature range, $\eta \simeq 0.6$, as noted in Sec. II A.

As CsI is added to liquid Cs, there is an increasingly strong deviation from the Korringa relation. This is illustrated in Fig. 7 which shows the observed $^{133}Cs$ relaxation rates $1/T_1$ and $1/T_2^*$ together with $(1/T_1)_{\text{Korringa}}$ plotted against the resonance shift. The relaxation is strongly enhanced for $x \lesssim 0.20$ and, in the region of the relaxation-rate peak, $1/T_2^*$ exceeds $(1/T_1)_{\text{Korringa}}$ by more than 2 orders of magnitude.

This striking breakdown of the Korringa relation is strong evidence against a "dilute-metal" model for Cs-CsI at low concentrations of Cs. The data indicate, in fact, that a fundamental transformation in the nature of the electronic states occurs for small concentrations of excess metal. Equations (11) and (12) show that an absolute increase in the relaxation rate accompanied by a decrease in electron concentration requires progressively longer correlation times. Longer correlation times, in turn, imply stronger electron localization as the metal concentration decreases. We shall return to a quantitative treatment of the localization process after discussing the specific structures of the electronic states.

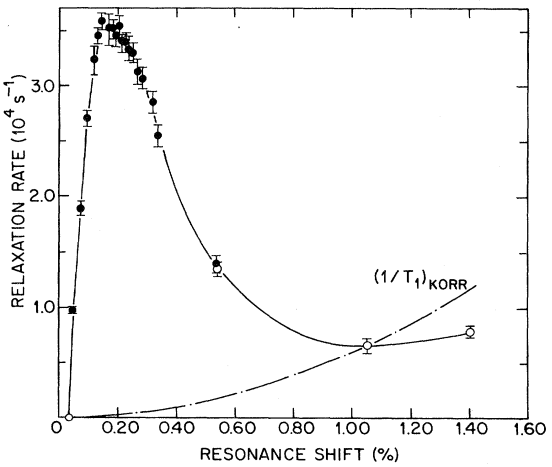


FIG. 7. Nuclear relaxation rates $1/T_2^*$ (solid circles) and $1/T_1$ (open circles) vs resonance shift for $^{133}Cs$ in Cs-CsI solutions at 640 °C. Solid line, guide to the eye through data points; dotted-dashed line, Korringa relaxation rate from Eq. (10).

*3. Structure of electronic states: Metallic and salt-rich limits*

*a. Metallic limit.* The state of strongly electronegative impurities in simple metals has been investigated extensively by Flynn and co-workers.[4,8–10] For sufficiently high electronegativity, an anion state is split off below the bottom of the conduction band. Screening of the negative charge then sets up strong perturbations in the conduction-electron system, leading to anomalously large impurity diamagnetic susceptibilities and strong spin-flip scattering.[8] These effects can be treated theoretically by a phase-shift analysis.

We have already cited structural evidence for the stability of the negative halogen ion in metal-rich alkali-metal—alkali-halide solutions. Ideally, such a state might be expected to yield a vanishing resonance shift for the halogen since conduction-electron charge is strongly repelled from the negative ion. The low value of the $^{127}$I shift shown in Fig. 2 clearly shows this tendency. However, the expulsion is incomplete since there is a substantial residual $^{127}$I shift in the metal. These states may be similar to states found at the bottom of the conduction band in crystalline CsI which are roughly 70% Cs 5*s* character and 30% I 6*s* character.[46]

*b. Salt-rich limit.* Strong breakdown of the Korringa relation shows that low concentrations of excess electrons in CsI are localized. The detailed structure of the localized states is not apparent *a priori*, however, and at least three possibilities must be considered: neutral Cs atoms, multisite localized states, and "*F* centers" (localization in place of an anion). We can distinguish among these by consideration of the average hyperfine coupling $\langle A \rangle$.

We assume that the concentration of localized spins equals the excess-metal concentration in our most dilute sample ($c_s = x$), and we employ Eq. (6) and the observed shift[47] to determine $\langle A \rangle$. The result for $^{133}$Cs, expressed as a probability density through Eq. (3), is

$$\langle |\Psi(\mathrm{Cs})|^2 \rangle = 0.56 \times 10^{25}\ \mathrm{cm}^{-3} .$$

This value and the corresponding result for $^{127}$I are shown in the first column of Table II. The average probability density for Cs is only about one-fifth of the atomic value,[48]

$$|\Psi(\mathrm{Cs})|^2_{\mathrm{atom}} = 2.58 \times 10^{25}\ \mathrm{cm}^{-3} ,$$

so that the experiment provides strong evidence against localization as a neutral atom.

Katz and Rice[49] proposed that localization in alkali-metal—alkali-halide solutions is a consequence of structural disorder, i.e., Anderson localization[50] dominates. However, a simple argument shows that the observed value of $\langle A \rangle$ is incompatible with this idea. The disorder-localized states are usually pictured as multisite states with amplitude $\phi_i \equiv f_i |\Psi(\mathrm{Cs})|^2_{\mathrm{atom}}$ on each ion. Since normalization of the wave function requires $\sum_i f_i \simeq 1$, the multisite model again leads to $\langle |\Psi(\mathrm{Cs})|^2 \rangle = \sum_i \phi_i \simeq |\Psi(\mathrm{Cs})|^2_{\mathrm{atom}}$, in disagreement with experiment.

Pitzer[51] proposed a quite different structure, namely that the electron is localized in the form of an *F* center. Thus the electron is considered to be localized in a site normally occupied by an anion and is coordinated by a number $n_1$ of cations. Unlike the crystalline *F* center, of course, $n_1$ can vary somewhat for different localized states and there is no unique local symmetry. Moreover, the complexes in the liquid would continually dissociate and reform due to the translational motion of individual ions.

Optical-absorption studies[14–16,52–55] of dilute concentrations of excess electrons provide considerable support for the *F*-center model. A strong band is observed at an energy similar to that of the corresponding crystal, but is shifted slightly by volume and structural changes associated with melting.[56] Recent studies of K-KCl show that this band may still be observed at concentrations of several atomic percent of excess K.[55]

The hyperfine-coupling values measured for Cs-CsI are in much better agreement with the *F*-center model than with the models discussed above in which the electronic charge is centered on one or more ions. To show this, we note that the average probability density of an *F*-center state on first-neighbor $Cs^+$ and second-neighbor $I^-$ ions would be approximately

$$|\Psi_F(\mathrm{Cs})|^2 \simeq (1/\bar{n}_1)\langle |\Psi(\mathrm{Cs})|^2 \rangle ,$$

$$|\Psi_F(\mathrm{I})|^2 \simeq (1/\bar{n}_2)\langle |\Psi(\mathrm{I})|^2 \rangle ,$$

where $\bar{n}_1$ and $\bar{n}_2$ are the average numbers of $Cs^+$ and $I^-$ ions, respectively, in the first two shells. Taking $n_1 = 4.5$ and $n_2 = 7.2$ (Ref. 57) leads to the values shown in the second column of Table II. Now the electron density for crystalline *F* centers can be measured directly for specific neighbor shells by electron-nuclear double-resonance (ENDOR) measurements. Experimental values are available for Cs in CsCl (Ref. 58) and I in KI (Ref. 59). To compare these with our results for Cs-CsI we make use of the fact that $d_1^3 |\Psi(R_i)|^2$ is roughly constant for the same ion in different alkali-halide crystals ($d_1$ is the near-neighbor distance).[59] For liquid CsI the value $d_1 = 3.85$ Å yields the results shown in the third column of Table II. Comparison with the crystal values (fourth column) shows that the $Cs^+$ first-neighbor electron densities are in excellent agreement and the $I^-$ values agree within about 30%. Although the specific values obtained for the liquid obviously depend on our choice of parameters, such as $\bar{n}_1$ and $\bar{n}_2$, the analysis supports the qualitative conclusion that excess electronic charge is localized in an empty "site" in the liquid structure.

The preceding analysis of hyperfine fields in the salt-rich range was based on the assumed presence of only a

TABLE II. Electron probability densities according to the *F*-center model for first-neighbor $^{133}$Cs and second-neighbor $^{127}$I nuclei.

| Nucleus | $\langle \lvert\Psi(R_i)\rvert^2 \rangle$ ($10^{24}$ cm$^{-3}$) | $\lvert\Psi_F(R_i)\rvert^2$ ($10^{24}$ cm$^{-3}$) | $d_1^3 \lvert\Psi_F(R_i)\rvert^2$ Liquid | Solid |
|---|---|---|---|---|
| $^{133}$Cs | 5.6±0.5 | 1.24 | 71 | 72[a] |
| $^{127}$I | 1.5±0.1 | 0.21 | 11.8 | 16.5[b] |

[a]Reference 58.
[b]Reference 59.

single localized paramagnetic species whose concentration $c_s$ is equal to the concentration of excess metal $x$. It is important to examine the validity of these assumptions, particularly in view of (i) clear evidence of spin-paired species from NMR measurements[25] in Na-NaBr, and (ii) estimates from optical-absorption[16] and electron-spin-resonance[60] intensities that $c_s \ll x$ for $x \gtrsim 0.01$ in Na- and K-based solutions. The magnetic susceptibilities[13,60] also indicate some spin pairing, particularly in the higher-concentration range, $x \gtrsim 0.05$. For $x \simeq 0.01$, the susceptibility per mole of excess metal in Cs-CsCl is within 10% of the value calculated for isolated $F$ centers with $c_s = x$, although experimental error and incomplete knowledge of the diamagnetism of the localized states introduce large uncertainties into both the experimental and calculated values.

A value $c_s \simeq 0.2x$ as reported[16] for $K_{0.01}KCl_{0.99}$ is not consistent with the $F$-center model and the observed hyperfine fields in Cs-CsI. Replacement of $c_s$ by $0.2x$ in Eq. (6) leads to a value of $\langle |\Psi(\mathrm{Cs})|^2 \rangle$ roughly equal to the atomic value and a value of $|\Psi_F(\mathrm{Cs})|^2$ which is about 5 times larger than the corresponding crystalline $F$-center value. Thus, although the optical and ESR spectral energies are in good agreement with the $F$-center model,[16,60] the intensities are not consistent with the NMR shifts. The latter require the $F$-center concentration to be $c_s \simeq x$.

There are at least two factors which may contribute to this apparent paradox. The first is that the concentration and stability of nonmagnetic (spin-paired) species seem to be quite different in different solutions. For example, the presence of such species in Na-NaBr provides an explanation for the anomalous behavior of the electrical conductivity in that solution at temperatures well below the critical point for liquid-liquid phase separation.[25] The conductivity anomaly disappears in Na solutions at higher temperatures and is not present at all in Cs solutions for which no phase separation occurs. As we discuss further in the next section, there is a clear difference in the behavior of the mobility in Na-NaBr and Cs-CsI. Thus, measurement of a reduced spin density by ESR for, e.g., excess Rb in NaCl-KCl eutectics,[60] may not be relevant to Cs-CsI. Regrettably, ESR has not been observed in Cs solutions, presumably because of extremely large linewidths.

A second important factor may be the existence of aggregates of $F$ centers which, viewed from nearest-neighbor nuclei, could produce NMR effects similar to those of isolated centers, but whose optical and ESR properties are quite different. That is, the optical and ESR lines may be due to a subset of localized states having particularly favorable properties, while the local fields at the nuclei, averaged over all possible environments, reflect a more general class of localized state. The roles of aggregates and metallic clusters in the region of the metal-nonmetal (MNM) transition are discussed further in Sec. V A 5.

#### 4. *Correlation times and electron transport*

We now consider the microscopic dynamics of the excess electrons as inferred from the nuclear relaxation. Since there is as yet no general theory of nuclear relaxation through the MNM transition we approach the problem from two limits: (i) itinerant (delocalized) electrons giving Korringa relaxation enhanced by strong electron-ion scattering, and (ii) well-localized ($F$-center) states whose lifetime determines the correlation time for nuclear relaxation.

For the itinerant limit, we use Eq. (11) to determine the concentration dependence of $\tau$. We first remark that the correlation time for pure liquid Cs is approximately $d/v_F$ where $d$ is the average interionic separation and $v_F$ is the Fermi velocity. Taking the free-electron value for $v_F$ yields $\tau(\mathrm{Cs}) = 7.8 \times 10^{-16}$ s.[61] To estimate the concentration dependence we assume that $N_e(E_F)$ varies according to free-electron theory and, from Eq. (11),

$$\tau(x) = \tau(\mathrm{Cs}) \frac{\eta(x)}{\eta(\mathrm{Cs})} \frac{N_e[E_F(x)]}{N_e[E_F(\mathrm{Cs})]} .$$

The resulting values of $\tau(x)$ plotted in Fig. 8 show the striking increase in $\tau$ responsible for breakdown of the Korringa relation. From the "Fermi times" $\tau \simeq 10^{-15}$ s characteristic of pure liquid Cs, $\tau$ increases to a typical "liquid structure time" $\tau \simeq 10^{-12}$ s for $x = 0.111$.

For the localized limit we make use of Eq. (12) with $c_s = x$ and, as is appropriate for $F$ centers,

$$\langle A^2 \rangle = (1/\bar{n}_1) \langle A \rangle^2 ,$$

where $\langle A \rangle$ is the hyperfine coupling previously determined from the shift analysis. The value of $\tau$ in our most dilute sample ($x \simeq 0.005$) is about $2 \times 10^{-12}$ s, and $\tau$ decreases rapidly with increasing metal content. The fact that the correlation time is never significantly longer than typical times for single-ion motion suggests strongly that $\tau$ should be interpreted as the correlation time for the hyperfine coupling, $A(t)$, rather than that for spin fluctuations, $S(t)$, even at the lowest metal concentrations. In the range $0.05 \lesssim x \lesssim 0.1$, the itinerant and localized models yield comparable values of $\tau$, although the concentration dependence is somewhat stronger for the itinerant model.

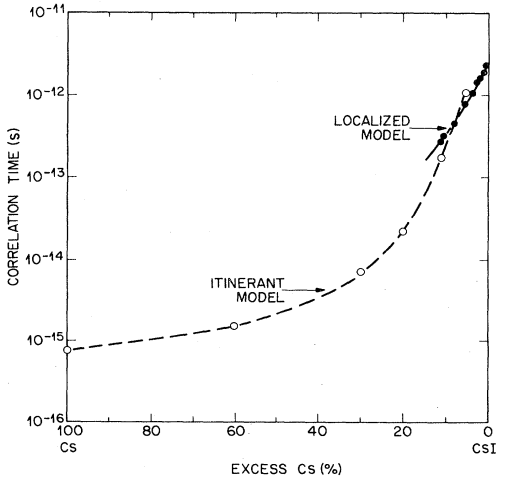


FIG. 8. Hyperfine-field correlation time vs composition for $^{133}$Cs in liquid Cs-CsI solutions at 640 °C. Open circles, itinerant model [Eq. (11)]; solid circles, localized model [Eq. (12)].

The strong concentration dependence of $\tau$ in the range of low metal concentration may be seen directly from the plot of $1/T_1$ vs $\Delta H/H$ in Fig. 7. Combining Eqs. (6) and (12) yields

$$\frac{1}{T_1}=\frac{2kT}{\hbar^2}\left[\frac{\gamma_n}{\gamma_e}\right]\frac{\langle A^2\rangle}{\langle A\rangle}\tau\frac{\Delta H}{H}\ , \tag{19}$$

so that if $\langle A^2\rangle/\langle A\rangle$ is independent of concentration, the slope of $1/T_1$ vs $\Delta H/H$ is proportional to $\tau$. The plot in Fig. 7 is strongly nonlinear, even for $x\simeq 0.01$, and it indicates rapidly decreasing values of $\tau$ in this range. This property of Cs-CsI solutions differs markedly from Na-NaBr, for which linear plots of $1/T_1$ vs $\Delta H/H$ show that the correlation time is independent of concentration nearly to the solubility limit for excess Na.[25]

The correlation times determined from the $^{133}$Cs relaxation rates provide the means for an independent test of the $F$-center model using the $^{127}$I relaxation data. Consider, for example, $x=0.055$, for which the rates are close to their peak values for both species. Taking $\tau=6.2\times10^{-13}$ s from the preceding analysis of the $^{133}$Cs rates and $\langle A^2\rangle_{127}=1/\bar{n}_2\langle A\rangle_{127}$ with $\bar{n}_2=7.2$,[57] we obtain for the magnetic contribution to the $^{127}$I rate

$$\left[\frac{1}{T_1}\right]_M=3.6\times10^3\ \mathrm{s}^{-1}\ \text{(calculated)}\ .$$

The experimental value of $(1/T_1)_M$ is obtained by subtracting the quadrupolar rate $(1/T_1)_Q$ from the observed rate. For $(1/T_1)_Q$ we use the observed relaxation in pure CsI. This yields

$$\left[\frac{1}{T_1}\right]_M=(3.75\pm0.20)\times10^3\ \mathrm{s}^{-1}\ \text{(experiment)}$$

The excellent agreement between the calculated and experimental values is an informative result since the calculated value depends linearly on the ratio $\bar{n}_1/\bar{n}_2$ and is independent of the fraction of spins $c_s$. Thus the number of $^{133}$Cs nuclei interacting with a given electron divided by the number of $^{127}$I nuclei is precisely the ratio of first to second coordination numbers expected for the $F$-center model. Other possible structures such as atomic states or clusters of metal atoms would give quite different values of this ratio.

We now consider the relationship between nuclear relaxation and the electrical conductivity. This relationship follows from the fact that for localized electrons or for strong-scattering itinerant electrons the hyperfine correlation time is determined by the microscopic mobility of the electrons. For the diffusive transport of strong-scattering itinerant electrons the conductivity is related to the Korringa enhancement by the approximate relation[30]

$$\sigma=\sigma_0/\eta\ . \tag{20}$$

Equation (20) is applicable for $\sigma\lesssim\sigma_0$ where $\sigma_0$ is a conductivity characteristic of scattering with a mean free path $\lambda$ equal to the average interatomic spacing $d$. This conductivity, the so-called Joffe-Regel conductivity,[62] is roughly constant for liquid systems and its value lies in the range 1000–3000 $(\Omega\,\mathrm{cm})^{-1}$.[63] Thus $\sigma_0$ is the value of the conductivity at which the onset of Korringa enhancement ($\eta>1$) occurs.

The data given in Fig. 7 show that Korringa enhancement occurs when $x\lesssim 0.6$. Recent measurements[12] of the dc conductivity yield $\sigma\cong 2000\ (\Omega\,\mathrm{cm})^{-1}$ at this composition, in good agreement with the prediction of Eq. (20). The conductivity at the enhancement onset for Cs-CsI also agrees well with values measured previously for Te-based semiconducting liquid alloys.[50] Thus we conclude that electronic transport in Cs-CsI is governed by weak-scattering transport ($\lambda>d$) for $x>0.6$ and by diffusive strong-scattering transport for $x\lesssim 0.6$. The lower-concentration limit of the strong-scattering range is determined by the metal-nonmetal transition which lies roughly in the range $0.05\lesssim x\lesssim 0.20$.

For the conductivity in the localized limit we write

$$\sigma_e=n_e\frac{e^2\langle a^2\rangle}{6kT}\frac{1}{\tau} \tag{21}$$

and assume that the hyperfine correlation time is equal to the residence time of an electron in a single localized state. In Eq. (21), $\sigma_e$ is the electronic contribution to the total conductivity $\sigma_{\mathrm{tot}}$ and it is obtained by subtracting the ionic contribution assumed to be the same as for pure CsI, i.e., $\sigma_e=\sigma_{\mathrm{tot}}-\sigma_{\mathrm{CsI}}$. The only unknown parameter in Eq. (21) is $\langle a^2\rangle$, the mean-square jump distance. Our experimental values of $\tau$ from NMR and a constant value $\langle a^2\rangle^{1/2}=21.4$ Å yield a good fit of Eq. (21) to the dc conductivity data of Sotier, Ehm, and Maidl[12] for $x\lesssim 0.10$.[64] Similar values ($\langle a^2\rangle^{1/2}\simeq 20$ Å) were found previously for Na-NaBr and Cs-CsCl.[23,25]

### 5. *Metal-nonmetal transition*

The foregoing analysis of NMR shifts and relaxation rates has led us to a reasonably complete picture of the electronic structure and dynamics in various ranges of concentration for Cs-CsI solutions. At low excess-metal concentrations, localized states form with structures resembling $F$ centers. The lifetimes of these states in the dilute limit are of the same order as single-ion-diffusion times, suggesting that the lifetime of the electronic state is limited by the lifetime of a favorable configuration of ions. When a localization site dissipates, an electron typically moves $\sim$20 Å before a new localized state is formed. For metal concentrations of a few atomic percent, the states are strongly interacting, the mobility decreases rapidly with concentration, and the electrons move significantly more rapidly than the underlying ionic structure. At still higher concentrations, the states become metallic in character and transport is of the diffusive strong-scattering type. Above about 60 at.% metal, the system becomes a nearly-free-electron metal. In this range the I is ionized and scatters electrons with a mean free path exceeding the average separation between $Cs^+$ ions. The rate of translational electron motion, measured by the correlation time $\tau$, increases continuously from "liquid-state" motions on the picosecond time scale at low metal concentrations to the Fermi-velocity motions on the femtosecond scale in the NFE limit.

The most difficult aspect of this problem remains a de-

tailed understanding of the MNM transition itself. A range of concentrations exists in which the electrons move from their locations in "vacancies" or "defects" in the charge-ordered liquid structure to extended states whose amplitudes lie mainly on the $Cs^+$ ions. The concentration dependence of $\tau$ shown in Fig. 8 suggests that this transition lies in the range $0.05 \lesssim x \lesssim 0.20$. At the present stage of knowledge it is difficult to define the transition range more precisely.

Because the electron distribution shifts from a location mainly off the ions to one mainly on the ions, it is not sufficient to describe the localization-delocalization transition in terms of metallic-type states with a varying correlation length. Instead, we are led to consider discrete species whose concentrations and stabilities change rapidly in the transition range. Evidence for the importance of such species was found in the NMR data for salt-rich Na-NaBr solutions.[25] Those experiments revealed the presence of nonmagnetic, nonconducting species whose concentration increased with metal content until the liquid-liquid phase separation was reached. The dimer $Na_2$ and the negative ion $Na^-$ are examples of possible species. The effect of such species is to remove excess electrons from the conduction process while the mobility of the remaining electrons is constant at the liquid-state value ($\tau \sim 1$ ps). This observation implies that the nonmagnetic species are stable longer than a typical single-ion motional time in Na-NaBr.

In contrast, the strongly-concentration-dependent mobility in Cs-CsI can be understood in terms of similar species which are short lived compared with the liquid structure. Rapid equilibrium between $F$ centers and spin-paired species would enhance the mobility since electrons can localize at new sites after dissociation. If the spin-paired species are polyatomic, a minimum jump time for this type of process would be imposed by the time scale of vibrational motions, i.e., $10^{-14}$–$10^{-13}$ s. The spin pairing would not significantly reduce the apparent value of $c_s$ provided that the lifetime of the species is short compared with the $F$-center lifetime.

Formation of short-lived species provides a natural mechanism for the electrons to move from vacancies to atomic sites. Moreover, as Nicoloso and Freyland have proposed,[60] it is reasonable to expect simple polyatomic species such as $Cs_2$ to give way to higher aggregates of localized states and clusters of metal atoms as the transition is approached. New support for this concept is provided by observation of the onset of a polarization catastrophe around $x = 0.1$ in K-KCl solutions.[55] The presence of these complexes suggests that the MNM transition has some of the features of a percolation transition but, in addition, the dynamics of the structural units influence electron transport in an important way.

### B. CsI-I solutions

#### *1. Dilute CsI-I solutions*

As shown in Figs. 3 and 4, addition of small amounts of I to CsI produces large increases in the nuclear relaxation rates for $^{133}Cs$ and $^{127}I$. The effect is striking even though, for $^{133}Cs$, it is 3 orders of magnitude smaller than the corresponding effect of excess Cs. The increase in relaxation rate is sufficiently strong that it precludes interpretation of this effect as enhancement of the quadrupolar relaxation characteristic of pure CsI.

We show this by using Eq. (16) to estimate the quadrupolar relaxation rate that might be expected from formation of molecular complexes associated with excess I. Such complexes would enhance the relaxation rate by lengthening the correlation times for the local electric field gradient as they slowly rotate. Taking a typical value[65] for $^{133}Cs$, $e^2qQ/\hbar \simeq 1.0 \times 10^6$ rad s$^{-1}$ and an estimated molecular reorientation time $\tau \simeq 10^{-10}$ s, we find $(1/T_1)_Q \sim 1$ s$^{-1}$. This is roughly 1 order of magnitude larger than the observed rate in pure CsI. However, the above estimate would apply only if *all* the $^{133}Cs$ nuclei were in complexes, whereas we observe rates exceeding 10 s$^{-1}$ with only 2 at. % excess I. Since most of the $^{133}Cs$ must remain as dissociated ions in such dilute solutions, the quadrupolar mechanism is incapable by a wide margin of explaining the observed increase in the $^{133}Cs$ rate. A similar analysis of the $^{127}I$ relaxation leads to the same conclusion.

The preceding argument and the evidence from the relaxation rates in $RbI_3$ discussed in Sec. IV B leads to the conclusion that the relaxation process associated with excess I is magnetic in origin. An obvious possibility is suggested by the $F$-center model for excess Cs and the properties of excess halogen in alkali-halide crystals, namely that the paramagnetism is due to localized holes—the $V_K$ center. This center consists of a hole associated with two iodine atoms bonded to form the $I_2^-$ molecular ion. It is a classic example of the polaron effect. The hyperfine interaction with the localized hole would lead to much stronger relaxation for the $^{127}I$ nuclei than for the $^{133}Cs$ neighbors and indeed this is observed. The observable consequences are limited to the relaxation rates because the coupling is too weak to produce a measurable $^{133}Cs$ shift while the $^{127}I$ line broadens so rapidly with the addition of I that shift measurements were impossible.

The presence of paramagnetic $I_2^-$ has recently been confirmed independently by Nakowsky, Nicoloso, and Freyland.[21] They observed a paramagnetic susceptibility contribution which increases strongly with addition of iodine and on raising the temperature. These centers give a clear ESR signal at low iodine concentrations and an optical-absorption band close to the position known for $I_2^-$ in crystals and aqueous solutions.

To obtain a lower limit on the correlation time for the localized hole we use Eq. (12) with the I $5p^5$ atomic hyperfine value $A = 5.48 \times 10^{-18}$ ergs (Ref. 66) and an estimate of the concentration of I in our most dilute sample, $c_s \sim 0.003$. With these parameters, the measured $^{127}I$ relaxation rate corresponds to a correlation time of 1.5 ps, about the same as found for localized electrons with dilute excess Cs. However, as we discuss more fully in the following section, the temperature dependence of $1/T_1$ indicates that the magnetic species are in equilibrium with other nonmagnetic species. Thus the spin concentration must be substantially lower than the excess-I concentration and the correlation time is much longer than the estimated lower limit. This is reasonable since diatomic

ions should be more stable than the configurations of 4 to 6 dissociated ions which provide the environment for localization of electrons.

### 2. Concentrated CsI-I solutions

As higher concentrations of I are added to CsI the $^{133}Cs$ relaxation rate increases monotonically. The temperature dependence, magnitude, and comparison with $RbI_3$ all indicate that the dominant process is magnetic and that it results from hyperfine coupling to paramagnetic species whose concentration increases with increasing temperature.

Calculations of the liquidus curves of CsI led Rosztoczy and Cubicciotti[20] to propose that the dominant species in CsI-rich CsI-I solutions are $Cs^+$, $I^-$, and $I_3^-$. If this is correct, then the simplest reaction leading to a paramagnetic species is

$$I_3^- + I^- \rightarrow 2I_2^- \ . \tag{22}$$

At higher I concentrations additional reactions could become increasingly likely, i.e.,

$$2I^- + I_2 \rightarrow 2I_2^- \ , \tag{23}$$

$$2I_3^- \rightarrow 2I_2^- + I_2 \ . \tag{24}$$

Nakowsky *et al.* suggest that higher polyhalide anions of the form $I_{2n+1}^-$ may be present as well.[21]

Since the concentration of magnetic species is governed by the enthalpies of reaction for the above equilibria, a shift in the relative importance of reactions (22)—(24) might explain the gradual increase observed in the activation energy of the relaxation rate as the I content increases. However, it must be borne in mind that the $^{133}Cs$ relaxation rate is also dependent on a correlation time for association of $Cs^+$ and $I_2^-$ ions and the temperature dependence of this time may change with concentration.

## VI. SUMMARY

We summarize the findings of this investigation by answering, to the extent possible, the basic questions posed in the introduction to this paper. First, it is clear that low concentrations of excess electrons introduced into molten CsI are strongly localized. These states are similar to *F* centers and, in the dilute limit, the localization time is limited by the lifetime of a local configuration of ions. There is no evidence for localization due to the absence of long-range order. Excess I in CsI also produces localized paramagnetic states. The available data indicate that these are $I_2^-$ molecular ions. This species is the liquid-state analog of the $V_K$ center—a polaron consisting of a localized hole and a lattice distortion to form a dimeric pair.

As the concentration of excess Cs is increased, the microscopic mobility of the localized electrons increases rapidly. We suggest that this mobility enhancement is due to rapid equilibrium between localized electrons and short-lived species such as $Cs_2$ or $Cs^-$. In the MNM-transition range the hyperfine correlation time drops rapidly and continuously, and the transport evolves to strong scattering in itinerant states. Our experiments do not reveal the nature of the liquid structure in the transition range and this remains an important problem. Additional optical studies and neutron or x-ray scattering experiments in this range would be valuable.

In the metallic range, strong-scattering transport persists up to about 60 at.% excess Cs. For higher metal concentrations, the nearly-free-electron model becomes appropriate. In this range, I is highly ionized although the conduction electrons still have nonvanishing amplitudes at the I nuclei. The degree of I 6*s* character is comparable with that found at the bottom of the conduction band of crystalline CsI.

CsI-I solutions contain increasing concentrations of paramagnetic species as the I content is increased. For all compositions, the number of paramagnetic species increases with temperature and the temperature dependence can be represented by an activation energy. The evidence strongly suggests explanation in terms of chemical equilibria between magnetic species such as $I_2^-$ and nonmagnetic (spin-paired) species such as $I_3^-$ and $I_2$.

*Note added in proof.* The *F*-center model has received further support from recent molecular-dynamics calculations [M. Parrinello and A. Rahman, J. Chem. Phys. **80**, 860 (1984)]. It was shown that an electron released in molten KCl rapidly localizes and is coordinated by roughly four cations.

## ACKNOWLEDGMENTS

The authors wish to thank W. Freyland and N. H. Nachtrieb for several valuable discussions and for providing us with their respective experimental results prior to publication. We are also indebted to D. W. Murphy for making available his dry box for sample preparation and to W. A. Bonner and E. Berry for the use of a vacuum furnace for making No-$Al_2O_3$ seals.

*Present and permanent addresses: Fachbereich Physik Technik, FB06 Fachhochschule München, D-8000 München 2, West Germany and Physik Department, Technische Universität München, D-8000 München 2, West Germany.

[1]See, for example, N. F. Mott, *Metal-Insulator Transitions* (Taylor and Francis, London, 1974).

[2]M. A. Bredig, in *Molten Salt Chemistry,* edited by M. Blander (Interscience, New York, 1964), p. 367.

[3]H. Hoshino, R. W. Schmutzler, and F. Hensel, Phys. Lett. **51A**, 7 (1975).

[4]R. Avci and C. P. Flynn, Phys. Rev. Lett. **41**, 428 (1978); Phys. Rev. B **19**, 5967 (1979); **19**, 5981 (1979).

[5]J. D. Corbett, in *Fused Salts,* edited by S. Sundheim (McGraw-Hill, New York, 1964), Chap. 6.

[6]W. W. Warren, Jr., in *Advances in Molten Salt Chemistry,* edited by G. Mamantov and J. Braunstein (Plenum, New York, 1981), Vol. 4, p. 1.

[7]See, for example, *Advances in Molten Salt Chemistry,* Ref. 6, p.

43.
[8]C. P. Flynn and J. A. Rigert, Phys. Rev. Lett. **27**, 3656 (1973).
[9]C. P. Flynn and N. O. Lipari, Phys. Rev. Lett. **27**, 1365 (1971).
[10]C. P. Flynn, Phys. Rev. B **9**, 1984 (1974).
[11]N. H. Nachtrieb, C. Hsu, M. Sosis, and P. A. Bertrand, in *Proceedings of the International Symposium on Molten Salts,* edited by J. P. Pemsler, J. Braunstein, and K. Nobe (Electrochemical Society, Princeton, New Jersey, 1976), p. 506.
[12]S. Sotier, H. Ehm, and F. Maidl, in *Liquid and Amorphous Metals V,* edited by C. N. J. Wagner and W. C. Johnson (North-Holland, Amsterdam, 1984), p. 95.
[13]N. Nicoloso and W. Freyland, Z. Phys. Chem. (Frankfurt am Main), **135**, 39 (1983).
[14]J. F. Rounsaville and J. J. Lagowski, J. Phys. Chem. **72**, 1111 (1968).
[15]H.-J. Yuh, Ph.D. thesis, University of Chicago, 1981.
[16]W. Freyland, K. Garbade, H. Heyer, and E. Pfeiffer, J. Phys. Chem. (to be published).
[17]R. Fainchtein and J. C. Thompson, Bull. Amer. Phys. Soc. **28**, 419 (1983).
[18]H. Yokokawa, O. J. Kleppa, and N. H. Nachtrieb, J. Chem. Phys. **71**, 4099 (1979).
[19]H. Yokokawa and O. J. Kleppa, J. Chem. Phys. **76**, 5574 (1982).
[20]F. E. Rosztoczy and D. Cubicciotti, J. Phys. Chem. **69**, 1687 (1965).
[21]B. Nakowsky, N. Nicoloso, and W. Freyland, Ber. Bunsenges. Phys. Chem. (to be published).
[22]S. Sotier and W. W. Warren, Jr., J. Phys. (Paris) Colloq. **41**, C8-40 (1980).
[23]W. W. Warren, Jr. and S. Sotier, in *Proceedings of the Third International Symposium on Molten Salts,* edited by G. Mamantov, M. Blander, and G. P. Smith (Electrochemical Society, Princeton, New Jersey, 1981), p. 95.
[24]W. W. Warren, Jr., in *Ionic Liquids, Molten Salts, and Polyelectrolytes,* edited by K.-H. Bennemann, F. Brouers, and D. Quitmann (Springer, Berlin, 1982), p. 28.
[25]W. W. Warren, Jr., S. Sotier, and G. F. Brennert, Phys. Rev. Lett. **50**, 1505 (1983).
[26]C. H. Townes, C. Herring, and W. D. Knight, Phys. Rev. **77**, 852 (1950).
[27]A. Abragam, *The Principles of Nuclear Magnetism* (Clarendon, Oxford, 1961), p. 306.
[28]J. Korringa, Physica (Utrecht) **16**, 601 (1950).
[29]U. El-Hanany, G. F. Brennert, and W. W. Warren, Phys. Rev. Lett. **50**, 540 (1983).
[30]W. W. Warren, Jr., Phys. Rev. B **3**, 3708 (1971).
[31]For a complete presentation of the quadrupole interaction see, for example, M. H. Cohen and F. Reif, in *Solid State Physics,* edited by F. Seitz and D. Turnbull (Academic, New York, 1957), Vol. 5, p. 321.
[32]Reference 25, p. 313.
[33]G. H. Fuller and V. W. Cohen, Nucl. Data Tables **A5**, 433 (1969).
[34]See, for example, C. P. Slichter, *Principles of Magnetic Resonance,* 2nd ed. (Springer, Berlin, 1978), p. 78.
[35]In one case a beryllia ceramic cell was used with equal success.
[36]W. G. Clark, Rev. Sci. Instrum. **35**, 316 (1964).
[37]W. Wolney Filho, R. L. Havill, and J. M. Titman, J. Phys. C **15**, 3617 (1982).
[38]See, for example, J. E. Enderby, J. Phys. C **15**, 4609 (1982).
[39]S. Biggin and J. E. Enderby, J. Phys. C **15**, L305 (1982).
[40]F. G. Edwards, J. E. Enderby, and D. I. Page, J. Phys. C **8**, 3483 (1975).
[41]Y. Derrien and J. Dupuy, J. Phys. (Paris) **36**, 191 (1975).
[42]N. S. Gingrich and Leroy Heaton, J. Chem. Phys. **34**, 873 (1961).
[43]G. Franz, W. Freyland, W. Gläser, F. Hensel, and E. Schneider, J. Phys. (Paris) Colloq. **41**, C8-194 (1980).
[44]J. Jal, doctoral thesis, Université Claude Bernard—Lyon I, 1981.
[45]See, for example, M. Shimoji, *Liquid Metals* (Academic, London, 1977), p. 162.
[46]Y. Onodera, J. Phys. Soc. Jpn. **25**, 469 (1968).
[47]To correct for the chemical shift, we take the paramagnetic shift to be the difference between the shift in the solutions and the shift in pure molten CsI.
[48]P. Kusch and H. Taub, Phys. Rev. **75**, 1477 (1949).
[49]I. Katz and S. A. Rice, J. Am. Chem. Soc. **94**, 4824 (1972).
[50]P. W. Anderson, Phys. Rev. **109**, 1492 (1958).
[51]K. S. Pitzer, J. Am. Chem. Soc. **84**, 2025 (1962).
[52]E. Mollwo, Nachr. Ges. Wiss. Göttingen, Math—Phys. Kl, Fachgruppe II, **1**, 203 (1935).
[53]D. M. Gruen, M. Krupelt, and I. Johnson, in *Molten Salts, Characterization and Analysis,* edited by G. Mamantov (Dekker, New York, 1969), p. 169.
[54]W. Schmidt and U. Schindewolf, Ber. Bunsenges. Phys. Chem. **81**, 585 (1977).
[55]W. Freyland, K. Garbade, and E. Pfeiffer, Phys. Rev. Lett. **51**, 1304 (1983).
[56]G. Senatore, M. Parrinello, and M. P. Tosi, Philos. Mag. B **41**, 595 (1980).
[57]H. A. Levy and M. D. Danford, in *Molten Salt Chemistry,* edited by M. Blander (Wiley-Interscience, New York, 1964), p. 109.
[58]F. Hughes and J. G. Allard, Phys. Rev. **125**, 173 (1962).
[59]H. Seidel and H. C. Wolf, in *Physics of Color Centers,* edited by W. B. Fowler (Academic, New York, 1963), p. 538.
[60]N. Nicoloso and W. Freyland, J. Phys. Chem. **87**, 1997 (1983).
[61]The correlation time for pure Cs could also be taken to be $\hbar N_e(E_F)$, as implied by Eq. (11). This yields a value of $\tau$ about a factor of 2 shorter than the one we have chosen, but is no more certain because of the approximate character of Eq. (11). The essential feature, the concentration dependence of $\tau$, is not affected by this scale factor.
[62]A. F. Ioffe and A. R. Regel, Prog. Semicond. **4**, 237 (1960).
[63]*Metal-Insulator Transitions,* Ref. 1, p. 27.
[64]The authors of Ref. 12 reported a slightly higher value, $\langle a^2\rangle^{1/2}=22.3$ Å, derived from an independent analysis of the NMR data. The discrepancy is consistent with experimental uncertainties in the correlation times.
[65]M. Emshwiler, E. L. Hahn, and D. Kaplan, Phys. Rev. **118**, 414 (1960).
[66]V. Jaccarino, J. G. King, R. A. Satten, and H. H. Stroke, Phys. Rev. **94**, 1798 (1954).